Experimental Generation of Riemann Waves in Optics: A Route to Shock Wave Control

Benjamin Wetzel,[1,2,*] Domenico Bongiovanni,[1] Michael Kues,[1] Yi Hu,[3] Zhigang Chen,[3,4] Stefano Trillo,[5] John M. Dudley,[6] Stefano Wabnitz,[7] and Roberto Morandotti[1,8,†]

[1]*Institut National de la Recherche Scientifique, Université du Québec, Varennes, Québec J3X 1S2, Canada*
[2]*School of Mathematical and Physical Sciences, University of Sussex, Sussex House, Falmer, Brighton BN1 9RH, United Kingdom*
[3]*The MOE Key Laboratory of Weak-Light Nonlinear Photonics, and TEDA Applied Physics Institute and School of Physics, Nankai University, Tianjin 300457, China*
[4]*Department of Physics and Astronomy, San Francisco State University, San Francisco, California 94132, USA*
[5]*Dipartimento di Ingegneria, Università di Ferrara, Via Saragat 1, 44122 Ferrara, Italy*
[6]*Institut FEMTO-ST, UMR 6174 CNRS-Université de Franche-Comté, 25030 Besançon, France*
[7]*Dipartimento di Ingegneria dell'Informazione, Università degli Studi di Brescia, and INO-CNR, via Branze 38, I-25123 Brescia, Italy*
[8]*Institute of Fundamental and Frontier Sciences, University of Electronic Science and Technology of China, Chengdu 610054, China*

(Received 3 May 2016; published 12 August 2016)

We report the first observation of Riemann (simple) waves, which play a crucial role for understanding the dynamics of any shock-bearing system. This was achieved by properly tailoring the phase of an ultrashort light pulse injected into a highly nonlinear fiber. Optical Riemann waves are found to evolve in excellent quantitative agreement with the remarkably simple inviscid Burgers equation, whose applicability in physical systems is often challenged by viscous or dissipative effects. Our method allows us to further demonstrate a viable novel route to efficiently control the shock formation by the proper shaping of a laser pulse phase. Our results pave the way towards the experimental study, in a convenient benchtop setup, of complex physical phenomena otherwise difficult to access.

DOI: 10.1103/PhysRevLett.117.073902

The formulation of conservation laws in terms of Riemann invariants [1] constitutes the foundation of the theory of classical shock waves [2–4]. In shock-bearing systems, the Riemann simple waves which allow describing the dynamics in terms of a single evolving Riemann invariant are crucial for understanding shock dynamics in different areas [5–7] and for the formulation of a modulation theory [8,9]. Yet Riemann waves (RWs) and their importance in terms of applications have been so far overlooked. In this Letter, we show that RWs can be conveniently observed in the context of a universal envelope equation, namely, the defocusing nonlinear Schrödinger equation (NLSE), which applies to nonlinear fiber optics [10–12], plasmas [13], Bose-Einstein condensates [14], and ocean wave dynamics [15–17]. Specifically, we consider an optical pulse envelope propagating in a fiber featuring strong nonlinearity and weak (normal) dispersion. In this regime, the NLSE is known to reduce to a 2×2 conservation law ruling wave propagation in shallow water (or isentropic gas dynamics), the so-called nonlinear shallow water equations [5,18–20]. Here we go further and demonstrate that, by suitably shaping the temporal profile of the pulse phase, we are able to experimentally generate RWs and control their breaking dynamics. The dynamical evolution of such RWs is fully described in terms of a single effective real variable (either one of the two Riemann invariants or the envelope modulus) obeying a remarkably simpler universal equation, namely, the inviscid Burgers equation (IBE) [2,21]. Although widely used as a paradigm for shock waves in a variety of physical [22–25] and socioeconomics [26] phenomena (with ramifications into turbulence [27–29]), to our knowledge the IBE still lacks a quantitative and controllable experimental comparison with theoretical predictions. Indeed, most physical systems exhibit higher-order effects that hinder its applicability, calling for the inclusion of additional terms (i.e., modified Burgers equations) [24,29]. Therefore, on one hand, our results establish nonlinear fiber optics as an effective and versatile environment to study the IBE dynamics in a convenient experimental setup. On the other hand, we also demonstrate that reshaping an arbitrary optical pulse into a RW can be exploited as a flexible means to effectively control the shock formation, in terms of both the associated temporal pulse profile and the shock distance along the fiber.

In the framework of nonlinear optics, a pulse with an envelope $A(z,T)$which propagates in an optical fiber with a nonlinear Kerr coefficient γ and group velocity dispersion β_2 follows the NLSE (given here in the form typically used for fiber optics [10,11]):

$$i\frac{\partial A}{\partial z} - \frac{\beta_2}{2}\frac{\partial^2 A}{\partial T^2} + \gamma|A|^2 A = 0, \tag{1}$$

where z is the propagation distance and T is the time coordinate in the comoving frame of the pulse. Let us now consider the transformation of an arbitrary optical pulse into a Riemann wave $A_{\mathrm{RW}}(z,T)$. To produce a RW, it is necessary to introduce an instantaneous frequency profile (chirp [10]) that is a scaled replica of the amplitude (or, in other words, the phase derivative is proportional to its amplitude) [19,20]. In the particular case where a Riemann pulse (with duration T_0 and peak power P_0) propagates in a fiber with normal dispersion ($\beta_2 > 0$), such that the dispersion length $L_D = T_0^2/\beta_2$ is much longer than the nonlinear length $L_{\mathrm{NL}} = (\gamma P_0)^{-1}$, the proportionality relation between the amplitude and chirp is preserved during propagation so that

$$A_{\mathrm{RW}}(z,T) = |A_{\mathrm{RW}}(z,T)| e^{\mp i 2\sqrt{\gamma/\beta_2}\int_{-\infty}^{T}|A_{\mathrm{RW}}(z,T')|dT'}. \quad (2)$$

More importantly, under these conditions [18], the evolution of the pulse amplitude (and chirp) in the fiber, which is described by the NLSE, can be well approximated until the shock point by the IBE [20], namely,

$$\frac{\partial|A_{\mathrm{RW}}|}{\partial z} \pm 3\sqrt{\gamma\beta_2}|A_{\mathrm{RW}}|\frac{\partial|A_{\mathrm{RW}}|}{\partial T} = 0. \quad (3)$$

Physically, IBE propagation is associated with pulse envelope steepening and eventually the formation of a so-called gradient catastrophe, where amplitude derivatives tend to infinity, leading to a characteristic shock wave behavior [2–4] (either at the trailing or leading edge of the Riemann pulse, depending on the sign of the chirp profile). Note that the shock dynamics of RWs is intrinsically different from the effect of pulse steepening arising from the frequency dependence of the nonlinearity in optical fibers [10,22]. In the IBE framework, the shock develops from the action of both nonlinearity and dispersion on the specifically prepared Riemann pulse, thus enabling a versatile and controlled shock formation. Indeed, the propagation of a Riemann pulse corresponds to a particular case of purely unidirectional energy flow [20], whose parametric representation can be readily obtained by the method of characteristics [2,4]. For the IBE evolution, the characteristic lines T_{Ci} (mapping the energy flow direction) extend from certain given points T_i (at $z = 0$) and can be analytically calculated for any arbitrary input pulse $A_{\mathrm{RW}}(0,T)$:

$$T_{Ci}(z,T_i) = T_i \pm 3\sqrt{\beta_2\gamma}|A_{\mathrm{RW}}(0,T_i)|z. \quad (4)$$

This energy flow representation highlights how high-density regions move with a different speed with respect to the low-density counterparts, until a multivalued solution (or shock) appears where these characteristic lines intersect. The shock distance z_B can thus be analytically predicted as $z_B = (3\alpha\sqrt{\gamma\beta_2})^{-1}$, with $\alpha = \max|\partial|A_{\mathrm{RW}}(0,T)|/\partial T|$.

Despite the simple form of the IBE, exciting a solution of Eq. (3) in a controllable fashion, as earlier theoretically proposed for dark spatial beams [19], remained so far unachieved in experiments. The challenge originates from the requirement of a precise control of the chirp profile and of the longitudinally invariant and well-characterized medium properties. In fact, although several wave-shaping-based experiments have recently been reported in hydrodynamics [16,17,30,31], there is an inherent difficulty in controlling the initial conditions in fluids and gases; moreover, dissipative effects and viscosity have so far precluded the clear and controlled observation of IBE dynamics and associated RW shock phenomena [3,22,24,29,32,33]. In contrast, arbitrary input optical waveforms can nowadays be synthesized by advanced pulse-shaping techniques [34]. This allows us to conveniently excite optical Riemann pulses and to compare experimental studies of pulse steepening and shock formation with analytical predictions using minimal approximations.

We first present in Fig. 1 numerical results illustrating Riemann pulse propagation in 2 km of optical fiber (with $\beta_2 = 0.8397\ \mathrm{ps^2\,km^{-1}}$ and $\gamma = 11.7\ \mathrm{W^{-1}\,km^{-1}}$ at 1550 nm). Specifically, Fig. 1(a) shows split-step NLSE simulations [10,11] for an input Riemann pulse given by Eq. (2), with a positive chirp and a Gaussian amplitude: $|A_R(z=0,T)| = \sqrt{P_0}\exp(-T^2/2T_0^2)$, where $P_0 = 0.89$ W and $T_0 = 2.7$ ps ($\Delta\tau_{\mathrm{FWHM}} = 1.665T_0 = 4.5$ ps). We can see the progressive steepening of the pulse trailing edge until $z = 500$ m, where a near-vertical front is formed (see also Ref. [35]). Remarkably, the Riemann pulse evolution is, before the shock onset, well described by the IBE and follows the direction of the energy flow as analytically predicted by the characteristic lines (white). The point where these lines intersect corresponds to the shock position, whose distance is correctly predicted from the IBE as $z_B = \sqrt{e}/3\sqrt{L_D L_{\mathrm{NL}}} = 500$ m. Additionally, Figs. 1(b) and 1(c) compare the intensity and chirp profiles at selected distances, as determined from either NLSE simulations (dashed blue curve) or directly from the IBE (solid black curve). In essence, until the shock point, the profiles obtained from the NLSE or the IBE are indistinguishable, illustrating how the Riemann pulse maintains its proportionality between chirp and amplitude. For $z \geq 500$ m, however, the IBE approximation loses validity due to the increasing effect of dispersive regularization: Although unnoticeable in the power profile of the pulse (which lays on a null background [36,37]), chirp oscillations develop on its trailing edge as a typical signature of dispersive shock wave formation [9,14,32,33,38–40].

To experimentally observe RW dynamics, we use the setup illustrated in Fig. 2(a). An optical parametric oscillator (OPO, Spectra Physics Opal) emits a train of 260-fs-long pulses that are spectrally shaped in intensity and phase (via a commercial waveshaper, Finisar 4000S) to generate

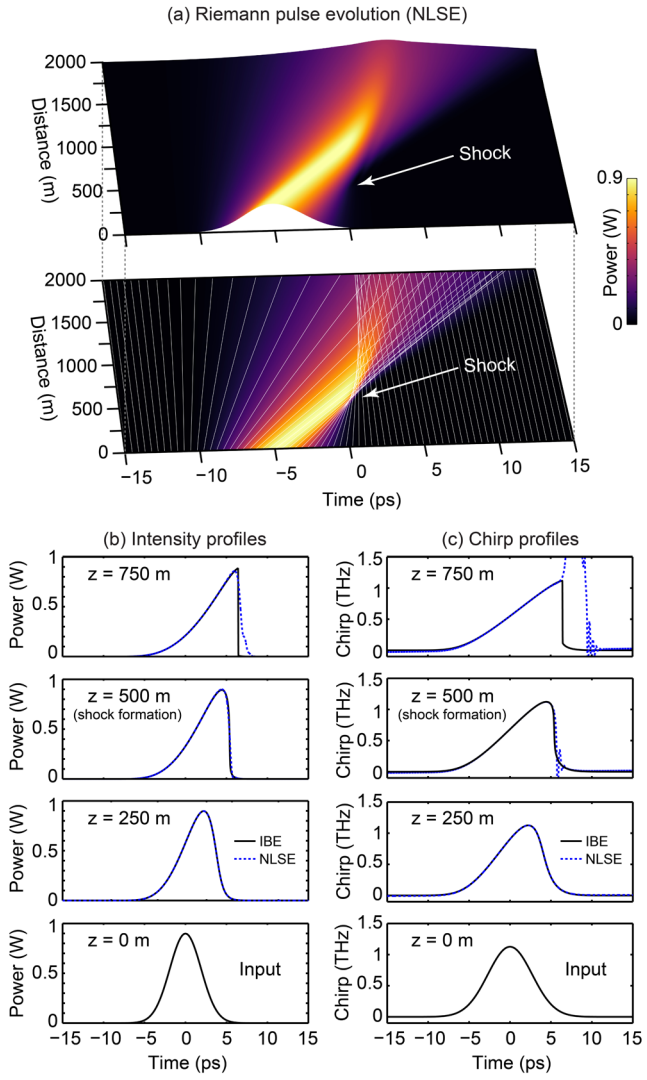

FIG. 1. (a) Intensity plot of Riemann pulse evolution in the fiber using the NLSE model (top). The projected pulse intensity (bottom) is compared with the characteristic lines obtained analytically from the IBE (white), showing shock formation at $z = 500$, where the characteristics intersect. Temporal profiles of the (b) intensity and (c) chirp are shown at selected distances, comparing IBE predictions (solid black curve) with NLSE simulations (dashed blue curve).

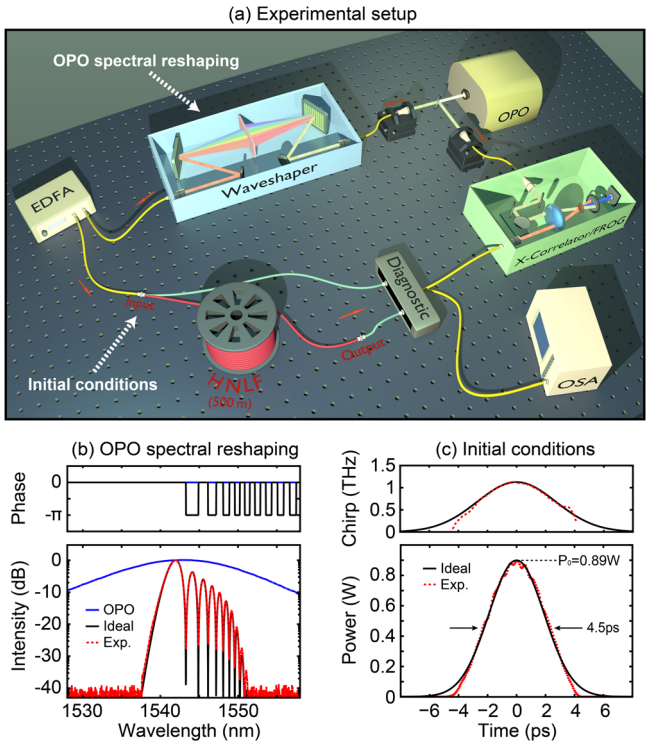

FIG. 2. (a) Optical setup. (b) An optical parametric oscillator (OPO) emits a train of Fourier-limited 260-fs-long pulses featuring a broad Gaussian spectrum (13.5 nm, blue line), which is reshaped in intensity and phase by a waveshaper, to yield an experimentally measured Riemann pulse spectrum (red dashed curve) compared with the target profile (solid black curve). (c) Following amplification in an erbium-doped fiber amplifier (EDFA), the Riemann pulse time domain characteristics, retrieved via XFROG characterization (red dashed curve), are compared with the target temporal profile (solid black).

the desired RW input. In Fig. 2(b), we represent the target spectral intensity and phase (black curve), the OPO spectrum (blue curve), along with the experimentally shaped spectrum (red curve), the latter characterized with an optical spectrum analyzer (OSA, ANDO AQ6317B). The pulses are optically amplified to reach a peak power of $P_0 = 0.89$ W and have a temporal FWHM of 4.5 ps before entering a highly nonlinear fiber (HNLF; see the parameters above). Figure 2(c) shows the time domain characteristics, after amplification, determined via a custom-built cross-correlation frequency-resolved optical gating (XFROG) setup [41]. Here we see identical chirp and amplitude profiles as expected for a Riemann pulse.

Experimental results for our analysis of pulse propagation in a 500-m-long HNLF are summarized in Fig. 3. Figures 3(b) and 3(c) show cross-correlation pulse profile measurements at the entrance and exit of the fiber, comparing experiments (red curve) with IBE predictions (black curve). The latter were extracted from the expected longitudinal propagation shown in Fig. 3(a). There is excellent agreement at the fiber output between experiments and IBE simulations; moreover, the cross-correlation measurements allow us to directly observe the development of the steepened trailing edge occurring at the shock point. These results in an optical system therefore provide, we believe, the first clear and quantitative experimental demonstration of IBE dynamics.

In a next step, we extend our study to a more general class of RWs via an additional tailoring of the spectral phase. Specifically, if $\tilde{A}_{\mathrm{RW}}(0,\nu)$ is the input Riemann pulse spectrum, by applying an additional quadratic spectral phase in the form of $\tilde{A}_{\mathrm{RW}\rho}(0,\nu) = \tilde{A}_{\mathrm{RW}}(0,\nu)\exp[i\rho(\nu-\nu_0)^2]$, we can generate a time-asymmetric input pulse (here ν_0 is the central frequency

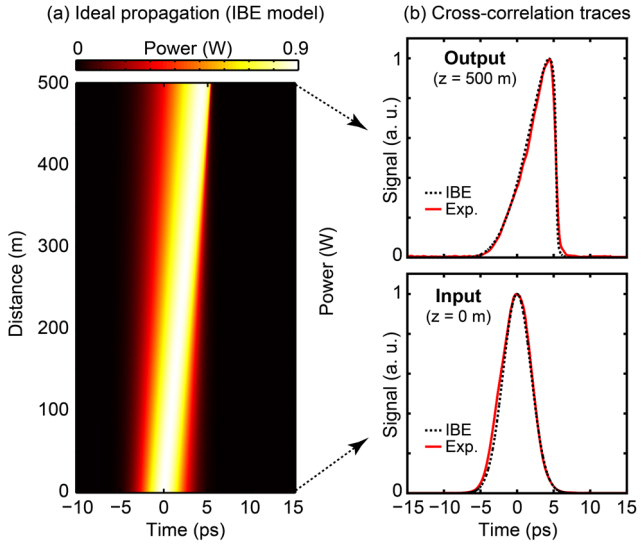

FIG. 3. (a) Riemann pulse propagation in 500 m of highly nonlinear fiber (IBE simulation). (b) Cross-correlation measurements at the entrance and the exit (500 m, at the shock point) of the fiber comparing experimental results (solid red curve) with the profiles expected from IBE simulations (black dashed curve).

and ρ is the quadratic phase coefficient). The degree of temporal asymmetry depends on ρ, while the pulse amplitude and chirp profiles still closely maintain their proportionality over a wide range of ρ values (i.e., for $|\rho| < 4$ ps^2, where the chirp average relative error compared to an ideal Riemann pulse remains below 10% and for which the IBE still remains approximately valid). Interestingly, this approach allows us to study a novel propagation regime of RWs where we can accurately tune the shock distance by means of a judicious choice of the initial phase (being physically analogous to an initial pulse propagation in a purely dispersive medium). Indeed, the powerful analytic description provided by the IBE predicts a linear rescaling of the asymmetric Riemann pulses' shock distance as a function of ρ.

An example of the concept of shock distance control via spectral phase tuning is illustrated in Fig. 4(a), showing simulation results and IBE characteristic lines for $\rho = \pm 4$ ps^2 (i.e., input pulses with opposite asymmetries). We can see how in both cases the evolution exhibits a progressive trailing edge steepening with quasiconstant peak power but with a shock distance that is shifted by about 450 m when the sign of the initial Riemann pulse asymmetry is reversed. In our experiments, we perform cross-correlation measurements of the output pulses at a distance of 500 m using these initial conditions, again obtaining an excellent agreement with simulations as can be seen in Fig. 4(b). Note that, even when we include attenuation in our NLSE simulations (or even higher-order dispersive and nonlinear terms [11]), the qualitative behavior is not changed for our parameters [42].

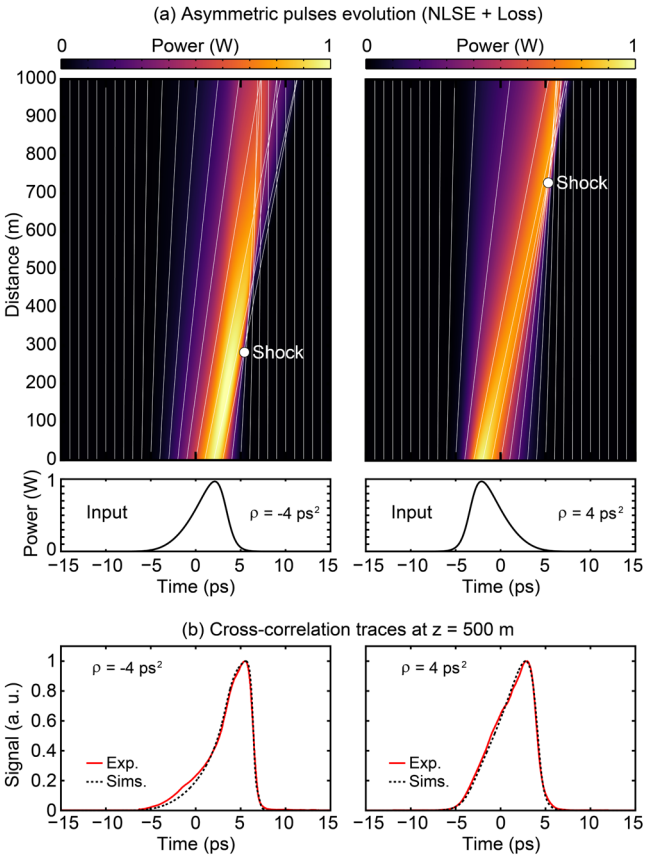

FIG. 4. (a) (Top panel) Numerical simulations and IBE characteristic lines (white) describing the evolution of input pulses of opposite asymmetry (bottom panel), obtained when quadratic spectral phases $\rho = \pm 4$ ps^2 were applied to the initial spectrum. In both cases, the pulse evolution yields to trailing edge steepening, although the predicted distances of shock formation are now shifted longitudinally (respectively, to 275 and 725 m). (b) The output cross-correlation profiles for $\rho = \pm 4$ ps^2, obtained at a fixed fiber length of 500 m, are measured experimentally (solid red curve) and compared with simulations (black dashed curve).

We can further assess the impact of RWs input temporal asymmetry by monitoring the output pulse characteristics. At a fixed distance of 500 m, we compute how varying ρ changes both the center of mass as well as the temporal and spectral pulse profiles at the fiber output [Figs. 5(a) and 5(b), respectively] [7]. In this case, one can readily observe a clear modification of the pulse steepened intensity profiles seen in Fig. 5(a) and the corresponding spectra shown in Fig. 5(b), both attesting to controllable shock distance rescaling. The experimental verification of these features can be conveniently obtained by measuring the output spectra as a function of ρ, as illustrated in Fig. 5(c). Here, our measurements are once more in excellent correspondence with the numerical results depicted in Fig. 5(b).

There are several conclusions to be drawn from this work. From a fundamental perspective, the ability to

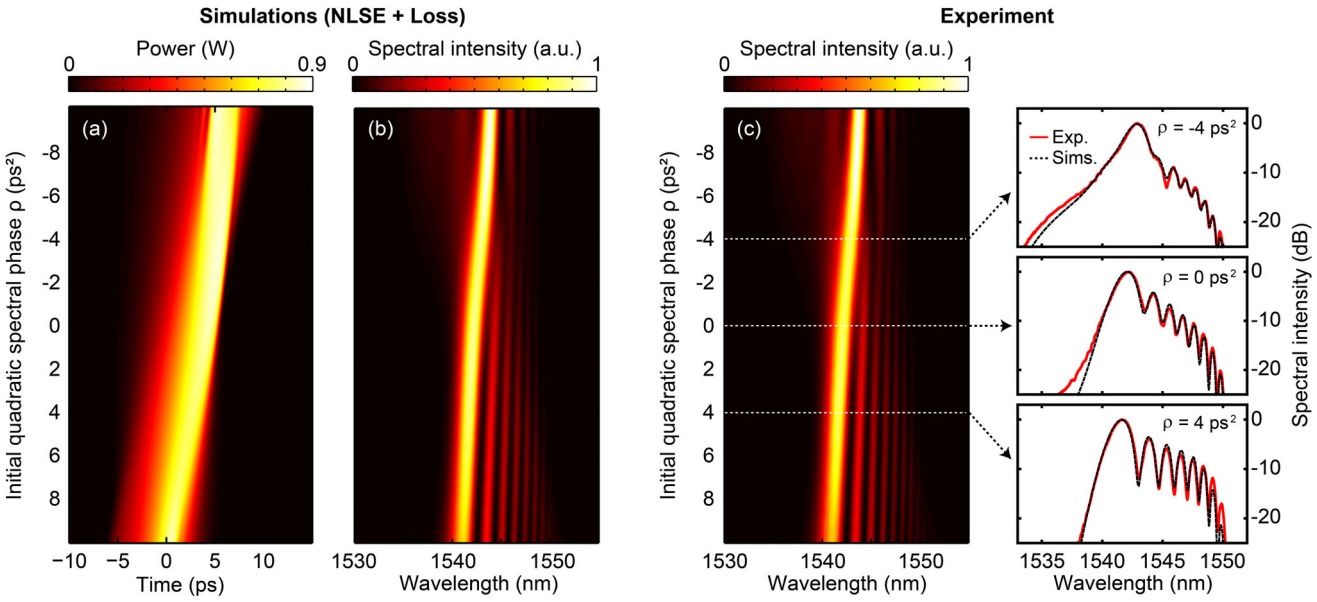

FIG. 5. (a) Simulated temporal and (b) spectral profiles at the HNLF output ($z = 500$ m) calculated as a function of ρ. (c) Experimental spectral intensity, observed under the same conditions used in (a) and (b) and measured at the fiber output with the OSA (for ρ increments of 0.4 ps^2). Output spectra for selected ρ values are shown in the right insets (logarithmic scale), where experiments (solid red curve) and numerical predictions (dashed black curve) are compared.

transform the description of wave propagation dynamics from a NLSE system to an IBE model of greatly reduced complexity represents a significant addition to the understanding of complex nonlinear dynamical systems. For instance, our results clearly demonstrate the temporal steepening of Riemann pulse envelopes in accordance with analytical predictions. Moreover, we optically solved the IBE for a range of different initial conditions, which underlines the potential and versatility of guided nonlinear optics for applications such as ultrafast analogue computing [43]. Finally, we proposed and demonstrated a flexible method for the shock distance control of arbitrary optical pulses, which opens up novel avenues towards (coherent) optical signal processing applications, including controlled nonlinear optical pulse retiming and real-time optical performance characterization.

We gratefully acknowledge very helpful discussions with Dmitry Pelinovsky, as well as the experimental support of Robin Helsten. This work was supported by the Natural Sciences and Engineering Research Council of Canada (NSERC) through the Strategic and Discovery Grants Schemes and from the MESI in Quebec. B. W. acknowledges the support from the People Programme (Marie Curie Actions) of the European Union's FP7 Programme under REA Grant Agreement INCIPIT (No. PIOF-GA-2013-625466). M. K. acknowledges support from FRQNT (Fonds de Recherche du Québec–Nature et Technologies) through the Merit Scholarship Program for Foreign Students Ministère de l'Éducation, de l'Enseignement Supérieur et de la Recherche du Québec) and funding from the European Union's Horizon 2020 research and innovation program under Marie Sklodowska-Curie Grant Agreement No. 656607. Z. C. acknowledges support from NSF and AFOSR. S. T. and S. W. acknowledge support from the Italian Ministry of University and Research (MIUR) (PRIN-2012BFNWZ2).

*benjamin.wetzel@emt.inrs.ca
†morandotti@emt.inrs.ca

[1] B. Riemann, Gott. Abh. Math. Cl. **8**, 43 (1860).
[2] G. B. Whitham, *Linear and Nonlinear Waves* (Wiley, New York, 1999).
[3] P. O. Krehl, History of Shock Waves, Explosions and Impact: A Chronological and Biographical Reference (Springer, New York, 2008).
[4] C. M. Dafermos, *Hyperbolic Conservation Laws in Continuum Physics* (Springer-Verlag, Berlin, 2010).
[5] A. V. Gurevich, A. L. Krylov, and G. A. El, Sov. Phys. JETP **74**, 957 (1992).
[6] L. A. Ostrovsky and K. R. Helfrich, Nonlinear Proc. Geophys. **18**, 91 (2011).
[7] D. Pelinovsky, E. Pelinovsky, E. Kartashova, T. Talipova, and A. Giniyatullin, JETP Lett. **98**, 237 (2013).
[8] A. V. Gurevich and L. P. Pitaevskii, Sov. Phys. JETP **38**, 291 (1974).
[9] G. A. El and M. A. Hoefer, Physica (Amsterdam) **333D**, 11 (2016).
[10] G. P. Agrawal, *Nonlinear Fiber Optics*, 5th ed. (Academic, New York, 2012).
[11] J. M. Dudley, G. Genty, and S. Coen, Rev. Mod. Phys. **78**, 1135 (2006).
[12] N. Akhmediev, J. M. Dudley, D. R. Solli, and S. K. Turitsyn, J. Opt. **15**, 060201 (2013).

[13] S. Dyachenko, A. Newell, A. Pushkarev, and V. Zakharov, Physica (Amsterdam) **57D**, 96 (1992).
[14] M. A. Hoefer, M. J. Ablowitz, I. Coddington, E. A. Cornell, P. Engels, and V. Schweikhard, Phys. Rev. A **74**, 023623 (2006).
[15] M. Onorato, S. Residori, U. Bortolozzo, A. Montina, and F. T. Arecchi, Phys. Rep. **528**, 47 (2013).
[16] A. Chabchoub, N. P. Hoffmann, and N. Akhmediev, Phys. Rev. Lett. **106**, 204502 (2011).
[17] A. Chabchoub, O. Kimmoun, H. Branger, C. Kharif, N. Hoffmann, M. Onorato, and N. Akhmediev, Phys. Rev. E **89**, 011002 (2014).
[18] Y. Kodama and S. Wabnitz, Opt. Lett. **20**, 2291 (1995).
[19] S. Malaguti, A. Corli, and S. Trillo, Opt. Lett. **35**, 4217 (2010).
[20] S. Wabnitz, J. Opt. **15**, 064002 (2013).
[21] Note that in several areas the inviscid Burgers equation is also known and referred as the Hopf equation.
[22] F. DeMartini, C. H. Townes, T. K. Gustafson, and P. L. Kelley, Phys. Rev. **164**, 312 (1967).
[23] Y. B. Zel'dovic, Astron. Astrophys. **5**, 84 (1970).
[24] J. L. Hammack and H. Segur, J. Fluid Mech. **65**, 289 (1974).
[25] D. Chowdhury, L. Santen, and A. Schadschneider, Phys. Rep. **329**, 199 (2000).
[26] S. Hodges and A. Carverhill, Econom. J. **103**, 395 (1993).
[27] A. Aceves, H. Adachihara, C. Jones, J. C. Lerman, D. W. McLaughlin, J. V. Moloney, and A. C. Newell, Physica (Amsterdam) **18D**, 85 (1986).
[28] G. Falkovich, K. Gawdzki, and M. Vergassola, Rev. Mod. Phys. **73**, 913 (2001).
[29] J. Bec and K. Khanin, Phys. Rep. **447**, 1 (2007).
[30] A. Chabchoub, N. Hoffmann, M. Onorato, G. Genty, J. M. Dudley, and N. Akhmediev, Phys. Rev. Lett. **111**, 054104 (2013).
[31] S. Fu, Y. Tsur, J. Zhou, L. Shemer, and A. Arie, Phys. Rev. Lett. **115**, 034501 (2015).
[32] J. A. Joseph, J. E. Thomas, M. Kulkarni, and A. G. Abanov, Phys. Rev. Lett. **106**, 150401 (2011).
[33] C. Conti, A. Fratalocchi, M. Peccianti, G. Ruocco, and S. Trillo, Phys. Rev. Lett. **102**, 083902 (2009).
[34] A. M. Weiner, Opt. Commun. **284**, 3669 (2011).
[35] See Supplemental Material at http://link.aps.org/supplemental/10.1103/PhysRevLett.117.073902 for a video illustrating the evolution of the Riemann wave spectrogram obtained using numerical simulations.
[36] A. V. Gurevich and A. L. Krylov, Sov. Phys. JETP **65**, 944 (1987).
[37] G. Xu, A. Mussot, A. Kudlinski, S. Trillo, F. Copie, and M. Conforti, Opt. Lett. **41**, 2656 (2016).
[38] J. E. Rothenberg and D. Grischkowsky, Phys. Rev. Lett. **62**, 531 (1989).
[39] J. Fatome, C. Finot, G. Millot, A. Armaroli, and S. Trillo, Phys. Rev. X **4**, 021022 (2014).
[40] G. Xu, D. Vocke, D. Faccio, J. Garnier, T. Roger, S. Trillo, and A. Picozzi, Nat. Commun. **6**, 8131 (2015).
[41] R. Trebino, *Frequency-Resolved Optical Gating: The Measurement of Ultrashort Laser Pulses* (Springer, New York, 2002).
[42] Note that, with the parameters of our fiber, the inclusion of losses of 0.8 dB/km is the predominant source of discrepancies compared to an ideal NLSE evolution but does not change the qualitative pulse evolution dynamics. The inclusion of third-order dispersion with $\beta_3 = 0.0234\ \mathrm{ps}^3\,\mathrm{km}^{-1}$ has an even lower impact on the pulse evolution while the effect of higher-order nonlinear terms is here negligible.
[43] D. R. Solli and B. Jalali, Nat. Photonics **9**, 704 (2015).